1521-0111/87/1/1–8$25.00
MOLECULAR PHARMACOLOGY

http://dx.doi.org/10.1124/mol.114.095661
Mol Pharmacol 87:1–8, January 2015

The Mitochondrial Complex V–Associated Large-Conductance Inner Membrane Current Is Regulated by Cyclosporine and Dexpramipexole

Kambiz N. Alavian, Steven I. Dworetzky, Laura Bonanni, Ping Zhang, Silvio Sacchetti, Hongmei Li, Armando P. Signore, Peter J. S. Smith, Valentin K. Gribkoff, and Elizabeth A. Jonas

Department of Internal Medicine (K.N.A., P.Z., S.S., H.L., E.A.J.) and Department of Neurobiology (E.A.J.), Yale University School of Medicine, New Haven, Connecticut; Division of Brain Sciences, Department of Medicine, Imperial College London, London, United Kingdom (K.N.A.); Department of Neuroscience, Imaging and Clinical Sciences, University G.d'Annunzio of Chieti-Pescara, Chieti-Pescara, Italy (L.B.); Knopp Biosciences LLC, Pittsburgh, Pennsylvania (S.I.D., A.P.S., V.K.G.); and Biocurrents Research Center, Marine Biological Laboratory, Woods Hole, Massachusetts (P.J.S.S.)

Received August 29, 2014; accepted October 20, 2014

ABSTRACT

Inefficiency of oxidative phosphorylation can result from futile leak conductance through the inner mitochondrial membrane. Stress or injury may exacerbate this leak conductance, putting cells, and particularly neurons, at risk of dysfunction and even death when energy demand exceeds cellular energy production. Using a novel method, we have recently described an ion conductance consistent with mitochondrial permeability transition pore (mPTP) within the c-subunit of the ATP synthase. Excitotoxicity, reactive oxygen species–producing stimuli, or elevated mitochondrial matrix calcium opens the channel, which is inhibited by cyclosporine A and ATP/ADP. Here we show that ATP and the neuroprotective drug dexpramipexole (DEX) inhibited an ion conductance consistent with this c-subunit channel (mPTP) in brain-derived submitochondrial vesicles (SMVs) enriched for F_1F_O ATP synthase (complex V). Treatment of SMVs with urea denatured extramembrane components of complex V, eliminated DEX- but not ATP-mediated current inhibition, and reduced binding of [^{14}C]DEX. Direct effects of DEX on the synthesis and hydrolysis of ATP by complex V suggest that interaction of the compound with its target results in functional conformational changes in the enzyme complex. [^{14}C]DEX bound specifically to purified recombinant b and oligomycin sensitivity–conferring protein subunits of the mitochondrial F_1F_O ATP synthase. Previous data indicate that DEX increased the efficiency of energy production in cells, including neurons. Taken together, these studies suggest that modulation of a complex V–associated inner mitochondrial membrane current is metabolically important and may represent an avenue for the development of new therapeutics for neurodegenerative disorders.

Introduction

The efficient regulation of cellular energy production by mitochondria is dependent on the integrity of the inner and outer mitochondrial membranes and the maintenance of the proton-motive force that drives the production of ATP by complex V, the ATP synthase complex (Caviston et al., 1998; Brand, 2005; Watt et al., 2010; Jonas et al., 2014). Under physiologic conditions, mitochondrial membranes contain a number of ion conductance pathways, including homologs of "classic" ion channels, with diverse regulatory and homeostatic functions, as well as conductance pathways that appear to be functionally expressed only under pathophysiological conditions (Pavlov et al., 2001; Kirichok et al., 2004; O'Rourke, 2004, 2007; Dejean et al., 2005; Bernardi, 2013; Elrod and Molkentin, 2013; Raffaello et al., 2013).

Mitochondrial dysfunction is particularly problematic in excitable cells, which have exceptional energy requirements (Nguyen et al., 1997; David and Barrett, 2003; Chouhan et al., 2012). In the case of neurons, their unique anatomic characteristics often require the physical translocation of mitochondria and metabolic precursors long distances along axons to distal synapses, providing numerous additional opportunities for disruption of critical energy supplies (Glater et al., 2006; Courchet et al., 2013; Sun et al., 2013; Sheng, 2014). Neuronal mitochondrial stress and injury result from environmental and genetic factors such as heteroplasmy, increasing the risk of cell death as increasing proportions of mitochondria become inefficient or unavailable (Albers and Beal, 2000; Nicholls, 2008). Large-conductance leak currents that disrupt mitochondrial osmotic gradients may develop

This work was supported by a grant from Knopp Biosciences LLC to Yale University School of Medicine, by the National Institutes of Health [Grants R01-NS045876 and R01-NS064967], and by the Italian Ministry of Health [Young Researchers Grant 2007 (Dementia with Lewy Bodies: New Diagnostic Markers and Therapeutic Implications)].
dx.doi.org/10.1124/mol.114.095661.

ABBREVIATIONS: ANOVA, analysis of variance; CsA, cyclosporine A; DEX, dexpramipexole; IB, isolation buffer; mPTP, mitochondrial permeability transition pore; OSCP, oligomycin sensitivity–conferring protein; SMV, submitochondrial vesicle.

during stress and contribute to mitochondrial dysfunction and bioenergetic inefficiency (Damiano et al., 2006; Rao et al., 2014). It had been shown previously that mitochondrial permeability transition may be brought on by calcium- or reactive oxygen species–induced opening of a nonselective inner membrane channel mitochondrial permeability transition pore (mPTP) (Petronilli et al., 1989; Szabo et al., 1992; Zorov et al., 2000; Bernardi, 2013). We have recently found that this conductance is located within the c-subunit of the ATP synthase (Alavian et al., 2014). We seek to understand more about the biophysical characteristics and reversibility of the opening of this channel and the possible implications for increasing bioenergetic efficiency by increasing the probability of channel closure. Understanding structural substrates for inhibition of these conductance pathways may provide insight into new avenues for the discovery of effective therapies for a variety of neuronal diseases.

Recently we presented evidence that cyclosporine A (CsA), a compound that is a known modulator of mitochondrial function (Szabo and Zoratti, 1991; Giorgio et al., 2009), and dexpramipexole (DEX) (Gribkoff and Bozik, 2008) inhibited stress- and injury-induced large-conductance currents recorded from whole neuronal mitochondria (Alavian et al., 2012). DEX is the nondopaminergic $R(+)$ enantiomer of the high-affinity dopamine agonist and Parkinson's disease therapeutic pramipexole (Mirapex; Boehringer Ingelheim Pharmaceuticals, Inc., Ridgefield, CT) (Gribkoff and Bozik, 2008). Pramipexole is neuroprotective by a nondopaminergic mechanism (Gu et al., 2004), likely involving inhibition of mitochondrial permeability transition pore (mPTP) (Cassarino et al., 1998; Sayeed et al., 2006). Because DEX is not a high-affinity dopamine agonist, its use avoids the side effects of dopaminergic agonists, and it is tolerated at clinical doses that are neuroprotective (Bozik et al., 2011). Mitochondrial effects of both drugs have not been completely characterized. DEX has been found to increase the efficiency of energy production in cells, including neurons, at concentrations that inhibit large-conductance mitochondrial currents (Alavian et al., 2012).

In the current study, we demonstrate that currents suppressed by CsA and DEX are located at the inner mitochondrial membrane and are also inhibited by ATP. We find that DEX binds to the oligomycin sensitivity–conferring protein (OSCP) and b-subunits of the F_1/F_O ATP synthase, suggesting that it may indirectly inhibit the c-subunit (mPTP) pore by producing a conformational change in complex V that places F_1 over the pore, inhibiting its conductance.

Materials and Methods

DEX. DEX was prepared by contract with Albany Molecular Research Inc. (Albany, NY; commercially available from Sigma-Aldrich, St. Louis, MO) and was determined to have chemical purity of >99.99% and enantiomeric ($R+$) purity relative to pramipexole of >99.95%.

Submitochondrial Vesicle Preparation. Preparations of submitochondrial vesicles (SMVs) were adapted from earlier methods (Sacchetti et al., 2013). The Lubrol-insoluble fraction (SMVs) was prepared from isolated mitochondria by resuspension in isolation buffer (IB) [250 mM sucrose, 20 mM HEPES (pH 7.2), 1 mM EDTA, and 0.5% bovine serum albumin] and combined with an equal volume of 1% digitonin on ice for 15 minutes. The pellet was washed twice in IB, resuspended in 200 μl of IB and 2 μl of 10% Lubrol PX (Calbiochem, San Diego, CA) on ice for 15 minutes, then layered onto IB and centrifuged at 39,000 rpm for 1 hour, followed by an IB wash. Final protein concentration was ~1–4 mg/ml of protein as determined by Pierce BCA Protein Assay (Thermo Scientific, Rockford, IL).

F_1 Removal from SMVs. F_1 subunits were removed from SMVs by adapting previously established methods (Pedersen et al., 1981). Sixty micrograms of SMVs per 1 ml of IB was treated with 1 ml of 6 M urea for 5 minutes on ice, then centrifuged at 21,000*g* for 10 minutes. The pellet was washed three times in IB (centrifugation at 21,000*g* for 10 minutes) and stored in IB.

[^{14}C]DEX Binding to SMVs. Urea-treated or control SMVs were incubated in [^{14}C]DEX (56 mCi/mmol; GE Healthcare UK, Pollards Wood, UK) overnight (4°C) in an agitator, then applied to a Centricon Centrifugal Filter Unit with Ultracel YM-10 membrane (Millipore Corp., Billerica, MA) and centrifuged at 4000*g* for 1 hour. SMVs were washed twice with IB. Filter units were incubated in Ultima Gold scintillation liquid (PerkinElmer Health Sciences, Inc., Waltham, MA) overnight. Samples were counted for ^{14}C with a Beckman Coulter LS 5000TD scintillation counter (GMI, Inc., Ramsey, MN).

[^{14}C]DEX Interaction with Heterologously Expressed F_1F_O ATP Synthase Subunits. The human open reading frame constructs for α, β, b, c, δ, d, ε, γ, and OSCP ATP synthase subunits, tagged with Myc or DDK (Flag) tags, were purchased from Origene Technologies (Rockville, MD). 293T cells were transfected with the above constructs, using the calcium phosphate method (Li et al., 2008). On day 3 post-transfection, the cells were lysed and the fusion proteins were bound to the EZview Red Anti-FLAG M2 Affinity Gel (Sigma-Aldrich), according to the manufacturer's protocol. The proteins were eluted from a portion of the samples, and the presence of the proteins on the beads was verified by immunoblot analysis, using mouse anti-Myc antibodies (Cell Signaling Technology, Danvers, MA). The protein-bound beads were incubated in the presence of [^{14}C]DEX overnight at 4°C in an end-over-end agitator. They were spun at 3000*g* in 0.45-μm Spin-X centrifugal devices (Corning Life Sciences, Tewksbury, MA) for 10 minutes. The samples were washed three times with phosphate-buffered saline, and the filter units were incubated in Ultima Gold scintillation liquid overnight. Samples were counted for ^{14}C using a Beckman Coulter LS 5000 TD scintillation counter.

Patch-Clamp Recordings from SMVs. Patch-clamp recordings were made from SMVs in intracellular solution (120 mM potassium chloride, 8 mM NaCl, 0.5 mM EGTA, and 10 mM HEPES; pH adjusted to 7.3) at room temperature (22–25°C). Pipettes (80–100 MΩ) were filled with the same solution; recordings were made using a HEKA 8 amplifier (HEKA Instruments, Bellmore, NY) with V_m held at positive voltages up to +180 mV. Data were recorded at 20 kHz and filtered at 500–1000 Hz. DEX (Knopp Biosciences LLC, Pittsburgh, PA) was prepared as a 10 mM aqueous stock and diluted in intracellular recording solution; CsA (Sigma-Aldrich) was prepared as an 8 mM stock solution in ethanol and diluted in buffer. Reagents were rapidly perfused into the recording chamber. Peak membrane conductance was measured as the peak amount of current (in picoamperes) from zero, converted to picosiemens by assuming a linear current-voltage relationship.

Western Blot Analysis. Western blot analysis was performed using standard protocols (Li et al., 2008). Primary antibodies were mouse anti–β-subunit 1:1000 (Mitosciences, Eugene, OR) and mouse anti–adenine nucleotide transporter 1:1000 (Santa Cruz Biotechnology, Dallax, TX).

Measurement of ATP Hydrolysis Using a Luciferin-Luciferase Assay. ATP hydrolysis in SMVs was measured with the BioVision Aposensor ATP Assay Kit in a 96-well plate with a plate reader (VICTOR3 Multilabel; PerkinElmer). SMVs were suspended in mitochondrial IB plus bovine serum albumin (0.5%) (Bonanni et al., 2006), ATP solution (final concentration, 0.5 mM), and 1 μl of reconstituted ATP-monitoring enzyme. To initiate, 100 μl of nucleotide-releasing agent containing Triton X was added and luminescence measured and displayed as percentage change in luminescence over

time. Three wells were used for each condition, repeated at least three times on different SMV isolations.

Measurement of ATP Hydrolysis Using an NADH Assay. ATP hydrolysis was also measured using an NADH-ATP-synthase kit (Mitosciences), according to the manufacturer's protocol with modifications (Lotscher et al., 1984). SMVs were added 20 minutes prior to addition of the reagent mix. The rate of change in fluorescence over time as NADH was oxidized was measured as a decrease in absorbance at 340 nm.

Kinetic ATP Synthesis Assay. Synthesis of ATP in liver mitochondria was measured using an ATP determination kit (Molecular Probes, Eugene, OR), supplemented with 1 mM sodium succinate and 500 nM rotenone. Assays were performed in 96-well microplates (Becton Dickinson, Franklin Lakes, NJ) in a final volume of 110 μl consisting of 10 μl of mitochondria (0.1 mg protein/ml final concentration), 10 μl of drug or control buffer, and 90 μl of ATP-determination reaction mixture. After a 5-minute recording of basal luciferase-generated luminescence, ADP (final concentration, 10 μM; 10 μl) was injected into each well. Luminescence was recorded every 6 seconds for 15–20 minutes.

Statistical Analyses and Curve Fitting. For comparisons involving two groups, paired or unpaired Student's t tests (two-tailed) were used. For more than two groups, one-way or two-way analyses of variance (ANOVAs) or two-factor multiple ANOVAs were performed; in the case of a significant F test, the P value is provided in the figure legend, and preplanned post hoc comparisons (Bonferroni-corrected t tests or Tukey's HSD test) were performed and significance levels displayed in figures and exact P values provided in the legends. Where possible, P values for tests are presented to two significant digits. All statistical analyses were performed using GraphPad Prism 5, InStat (GraphPad Software, Inc., La Jolla, CA) or SPSS (IBM Corporation, Somers, NY).

Results

Patch-Clamp Recordings of SMVs Containing F_1F_O ATPase Revealed an ATP-, CsA-, and DEX-Sensitive Leak Conductance. In a previous study (Alavian et al., 2012), patch-clamp recordings were made from whole mitochondria; drug-induced current inhibition induced by DEX and CsA recorded in those experiments could have reflected changes in mitochondrial currents localized at either or both the inner and outer mitochondrial membrane (Alavian et al., 2012). An increase in inner membrane leak conductance would be particularly effective at decreasing mitochondrial metabolic coupling. To test if the DEX- and CsA-inhibited conductance was expressed at the inner mitochondrial membrane, and was functioning directly as a "metabolic leak," we patch-clamped brain-derived SMVs. This preparation consists of isolated inverted inner membrane vesicles containing detergent-resistant mitochondrial components, and in particular F_1F_O ATP synthase (Chan et al., 1970; Sacchetti et al., 2013). In the absence of ATP, gigaohm seals were formed on SMVs and high levels of conductance (peak levels, 600–1200 pS) were recorded. Currents in SMVs were modestly enhanced by high [Ca^{2+}] and were inhibited by both DEX and CsA (Fig. 1, A and B). Maximal levels of inhibition by these

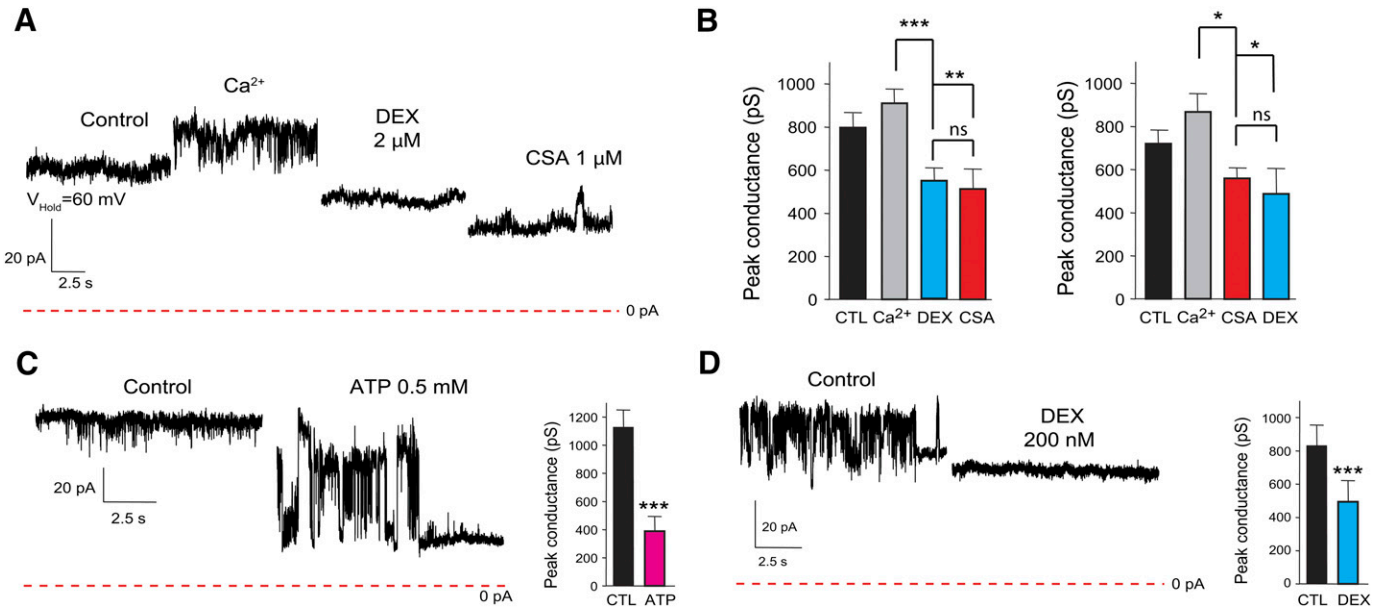

Fig. 1. DEX and CsA decreased conductance in SMVs. (A) Example patch-clamp recording from a brain-derived SMV; holding potential, +60 mV, before and after addition of the indicated agents to the bath (Ca^{2+} = 100 μM, DEX = 2 μM, CsA = 1 μM). (B) Histograms represent group data (mean ± S.E.M.) of peak conductance of experiments in (A). Current was measured from 0 pA and presented as peak conductance assuming a linear current-voltage relationship. (Left) Level of conductance before and after switching to high [Ca^{2+}], Ca^{2+} plus 2 μM DEX (n = 13 SMVs), followed by Ca^{2+}, DEX, and 1.0 μM CsA (n = 5 SMVs). One-way ANOVA, P = 0.0002; preplanned post hoc Bonferroni-corrected t tests, Ca^{2+} versus 2 μM DEX, P = 0.00041; Ca^{2+} versus CsA, P = 0.0048. (Right) Reversal of order of DEX and CsA addition: level of conductance in SMVs in control medium, after switching to high [Ca^{2+}], followed by Ca^{2+} plus 1.0 μM CsA (n = 5 SMVs), then Ca^{2+}, CsA, and 2 μM DEX (n = 3 SMVs). One-way ANOVA, P = 0.0043; preplanned post hoc Bonferroni-corrected t tests, Ca^{2+} versus CsA, P = 0.0196; Ca^{2+} versus DEX, P = 0.046. (C) Example SMV recording before and after addition of 0.5 mM ATP; holding voltage, +110 mV; discontinuous recording; ATP was added <1 minute prior to the break in the recording. Bar chart indicates group data (mean ± S.E.M.) for the effect of 0.5 mM ATP on peak conductance level (n = 9 SMVs, P = 0.0001, paired t test). (D) Example SMV recording before and after addition of 200 nM DEX; discontinuous recording; holding potential, +100 mV. Histograms indicate group data for the effect of 200 nM DEX on peak conductance level (n = 6 SMVs, P = 0.0003, paired t test). In all cases, recordings are discontinuous; addition of drugs occurred from 30 seconds to 10 minutes prior to recording the steady-state response of the drug at the given concentration. *$P < 0.05$; **$P < 0.01$; ***$P < 0.001$; ns, not significant.

compounds were approximately equal, and they showed only insignificant levels of additivity (Fig. 1B). The effects of the drugs were also observed in the absence of added Ca^{2+} (see all other figures), and the effects of DEX were reversible. ATP, a known blocker of mPTP as well as a metabolic modulator, also decreased peak membrane conductance of SMVs (Fig. 1C). The maximal effect of ATP was greater than the effect of DEX or CsA (Fig. 1, C and D), and both ATP and DEX decreased the conductance of SMV membrane patches in a concentration-dependent manner (Fig. 2, A and B). DEX was potent, with an EC_{50} = 111 nM, very similar to the previously published value obtained in whole, brain-derived mitochondria (Alavian et al., 2012), and the curve was, as previously observed for this compound, quite shallow, with a Hill slope of $<<1$. ATP was much less potent (EC_{50} = 224 μM), but the Hill slope was >1, and ATP was much more effective, consistently blocking a greater percentage of the total conductance.

DEX Modulated the Enzymatic Activity of Complex V. Interaction of DEX with inner mitochondrial membrane components resulted in current inhibition. We had previously observed a small but significant increase in ATP production in some cells in the presence of DEX, even when oxygen consumption rates were decreased or unaffected. This suggested the possibility that DEX directly interacted with complex V, an action that could concomitantly produce an alteration of its enzymatic function. Three different techniques were employed to measure the ability of complex V to hydrolyze or synthesize ATP in the presence and absence of DEX. SMVs can hydrolyze ATP (Alavian et al., 2011), and we found that DEX significantly enhanced ATP hydrolysis in SMVs in a concentration-dependent manner in an assay in which complex V enzymatic activity was estimated by the change in NADH signal (Fig. 3A); CsA also significantly enhanced ATP hydrolysis (Fig. 3A). In a different assay utilizing SMVs, DEX increased ATP hydrolysis, measured by ATP-luciferase levels in the medium, with an EC_{50} = 163 nM. The ATP synthase inhibitor oligomycin effectively inhibited ATP hydrolysis in both of these assays. In isolated liver mitochondria, where the presence of a proton gradient allows for ATP synthesis, DEX modestly increased ATP synthesis in response to an ADP pulse (Fig. 3B). The effect of DEX was significant and potent (EC_{50} = 166 nM), and like other measures of DEX's action, the concentration-response curve had a Hill slope of <1.

DEX Binding and Current Inhibition Were Reduced by Removal or Denaturation of F_1 or Other Extramembrane Components from the F_1F_O Mitochondrial ATP Synthase in SMVs. Complex V has an inside-out orientation in SMV membranes (Chan et al., 1970; Ko et al., 2003), with the F_1 head on the external side of the membrane. This

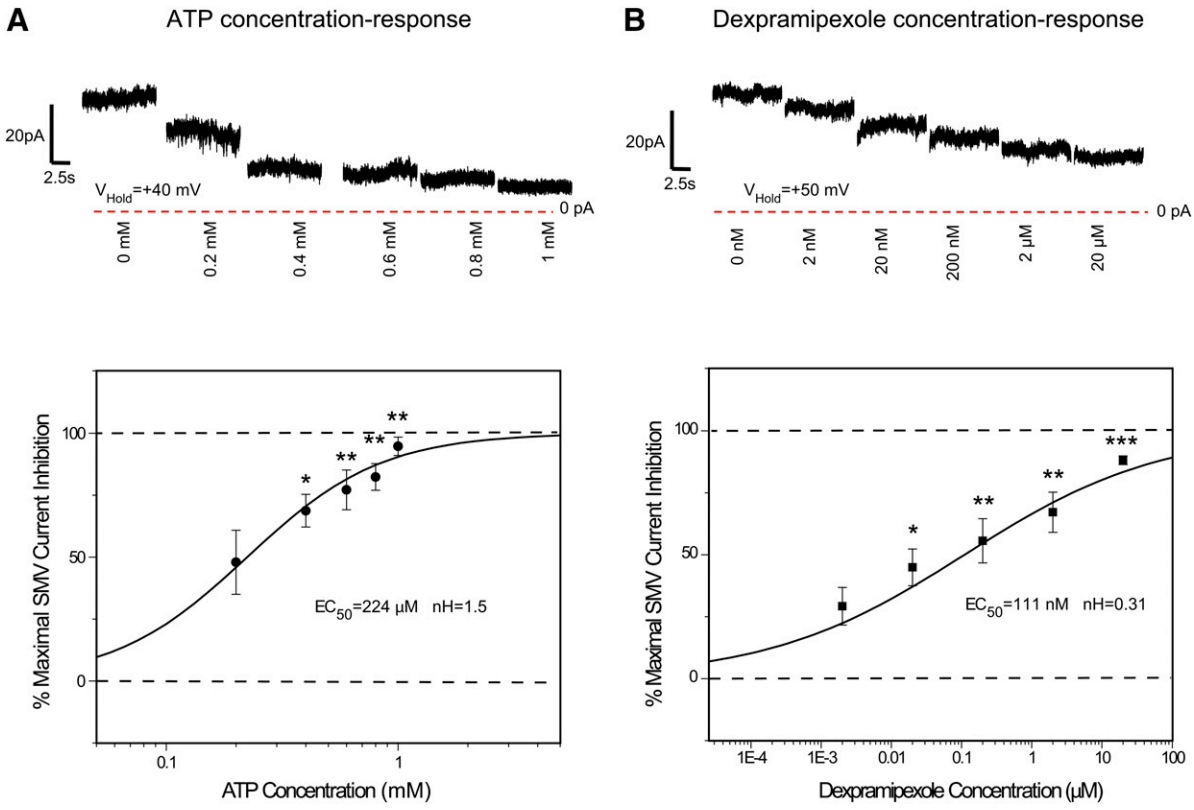

Fig. 2. Concentration-response relationship for the inhibition of currents in SMVs by ATP and DEX. (A, Top) Effect of ATP on peak conductance levels; holding potential, +40 mV. (Bottom) Group mean data and logistic fit estimate of the effect of ATP concentration on percentage maximal SMV current inhibition (n = 4 SMVs; EC_{50} = 224 μM; Hill slope = 1.5). One-way ANOVA, P = 0.0001; preselected post hoc Bonferroni-corrected t tests, control versus 0.4 mM ATP, P = 0.010; 0.6 mM, P = 0.0032; 0.8 mM, P = 0.0023; 1.0 mM, P = 0.0016. (B, Top) Effect of DEX on peak conductance levels in SMVs; holding potential, +50 mV. (Bottom) Group mean data and logistic fit estimate of the mean (±S.E.M.) percentage maximal current inhibition at different concentrations of DEX (n = 5 SMVs; EC_{50} = 111 nM; Hill slope = 0.31). One-way ANOVA, $P < 0.0001$; preselected post hoc Bonferroni-corrected t tests, control versus 20 nM DEX, P = 0.0375; 200 nM, P = 0.009; 2 μM, P = 0.0025; 20 μM, P = 0.0005. In all cases, recordings are discontinuous; addition of drugs occurred from 30 seconds to 5 minutes prior to recording the steady-state response. $^*P < 0.05$; $^{**}P < 0.01$; $^{***}P < 0.001$ versus control.

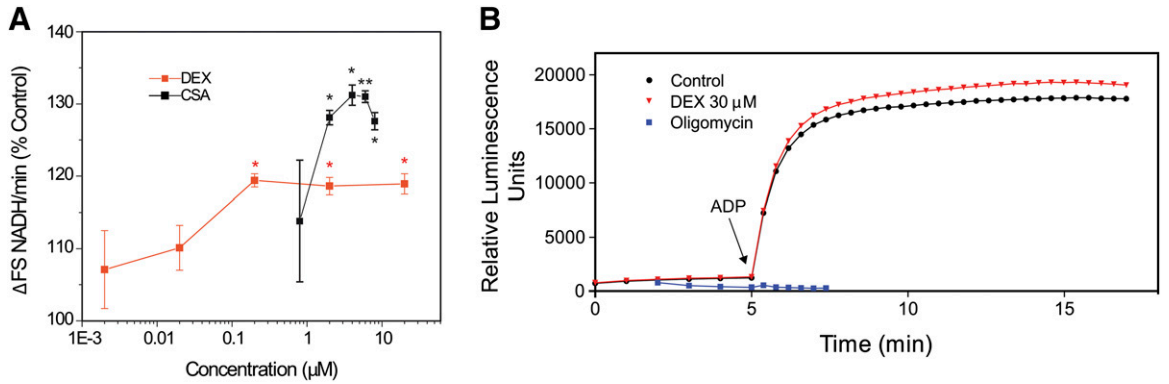

Fig. 3. DEX modulates complex V activity. (A) F_1F_O ATPase activity (ATP hydrolysis) in the presence of different concentrations of DEX (red squares) or CsA (black squares) shown as a function of the rate of decrease in NADH fluorescence and expressed as percentage of control; DEX, $n = 3$ determinations/point, one-way ANOVA, $P = 0.0014$; CsA, $n = 3$ determinations/point, one-way ANOVA, $P = 0.0002$. Pre-selected Bonferroni-corrected post hoc comparisons, control versus 200 nM DEX, $P = 0.0315$; 2 μM, $P = 0.0456$; 20 μM, $P = 0.0438$; control versus 2 μM CsA, $P = 0.0132$; 4 μM, $P = 0.010$; 6 μM, $P = 0.0096$; 8 μM, $P = 0.0152$. (B) ATP synthesis: change in ATP levels over time in liver mitochondria ($n = 3$ wells/point) following an ADP pulse using a dynamic luciferin-luciferase assay. All drugs added at time 0. $^*P < 0.05$; $^{**}P < 0.01$ versus control.

allowed us to examine the effects of urea treatment (see *Materials and Methods*), which removes/denatures non-membrane–residing components from protein supercomplexes and, in particular, the F_1 and associated components of complex V. Urea-treated SMVs were unable to perform ATP hydrolysis, and removal of the F_1 β-subunit was confirmed by Western blot immunoanalysis, whereas a known membrane-inserted component, the adenine nucleotide translocator, was unaffected (Fig. 4, A and B). These urea-treated SMVs still displayed leak conductance of similar magnitude under patch clamp (peak conductance, 600–1200 pS), but DEX no longer inhibited the conductance, suggesting that the presence of a non-membrane-inserted component was critical for DEX's effects (Fig. 4C). ATP, however, still very effectively decreased the leak conductance in the absence of F_1 (Fig. 4C). Finally, total binding of [^{14}C]DEX to SMVs was determined before and after treatment with urea. In three independent experiments, the total binding of [^{14}C]DEX was significantly reduced (mean reduction, 42%) with elimination of functional F_1 (Fig. 4D). These data demonstrate that a urea-sensitive component in SMVs was responsible for both binding of [^{14}C]DEX and DEX-regulated current inhibition.

Interaction of [^{14}C]DEX with Specific Subunits of Complex V. To further determine if the site of interaction of DEX resulting in inhibition of inner membrane current is localized to one or more subunits of complex V, individual subunits were heterologously expressed in 293T cells (Fig. 5A) and bound to affinity gels. The bound protein was used to directly test for the specific binding of [^{14}C]DEX. When incubated in [^{14}C]DEX, two subunits, b and OSCP, demonstrated levels of [^{14}C]DEX binding that were significantly greater than those incubated with the untransfected control cell lysate or other complex V subunits (Fig. 5B). Coincubation in "cold" DEX (100 μM) significantly reduced binding of these subunits to levels indistinguishable from untransfected controls, suggesting specific and competitive binding to subunits comprising the lateral stalk (stator) of the mitochondrial ATP synthase (Fig. 5C).

Discussion

Evidence has accumulated over the last decade strongly implicating mitochondrial dysfunction in a number of chronic neurodegenerative disorders (Chaturvedi and Beal, 2008).

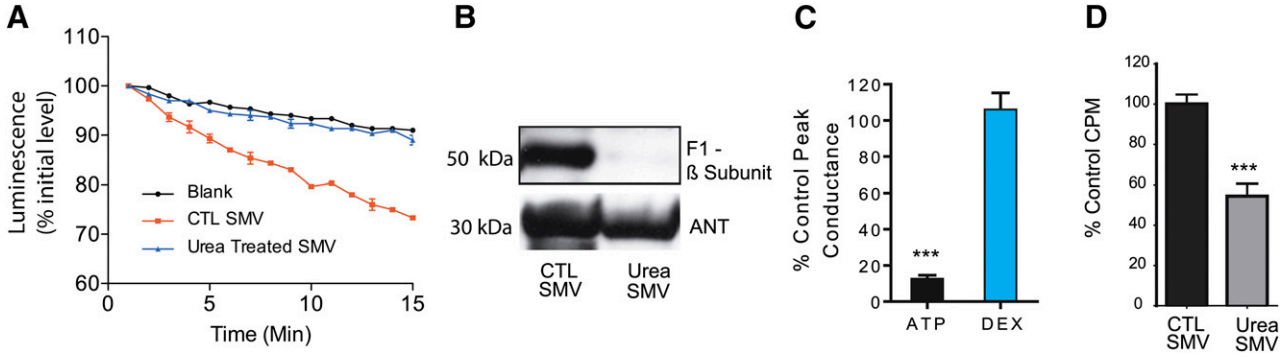

Fig. 4. Denaturation of extramembrane proteins in SMVs eliminated DEX- but not ATP-induced current inhibition. (A) Decrease in oxyluciferin luminescence levels indicating time-dependent decreases in ATP levels in the absence (Blank) and presence (CTL SMV) of SMVs and in the presence of urea-treated SMVs ($n = 3$ wells for each condition). (B) Immunoblot with an antibody against the F_1 β-subunit in protein from control SMVs or urea-treated SMVs. Identical protein concentrations were loaded in each well. Bottom shows adenine nucleotide translocator (ANT) protein level as a loading control. (C) Peak membrane conductance (percentage of control) of urea-treated SMVs in the presence of the indicated agents (ATP, 1.0 mM; DEX, 200 nM; $n = 7$ SMVs for ATP; $n = 6$ SMVs for DEX). Groups represent separate experiments; $P = 0.0028$ for ATP, unpaired t test. (D) Level of [^{14}C]DEX binding in SMVs treated with urea, relative to control SMV levels ($n = 15$ samples/condition; $P \leq 0.0001$, unpaired t test). $^{***}P < 0.001$ versus control.

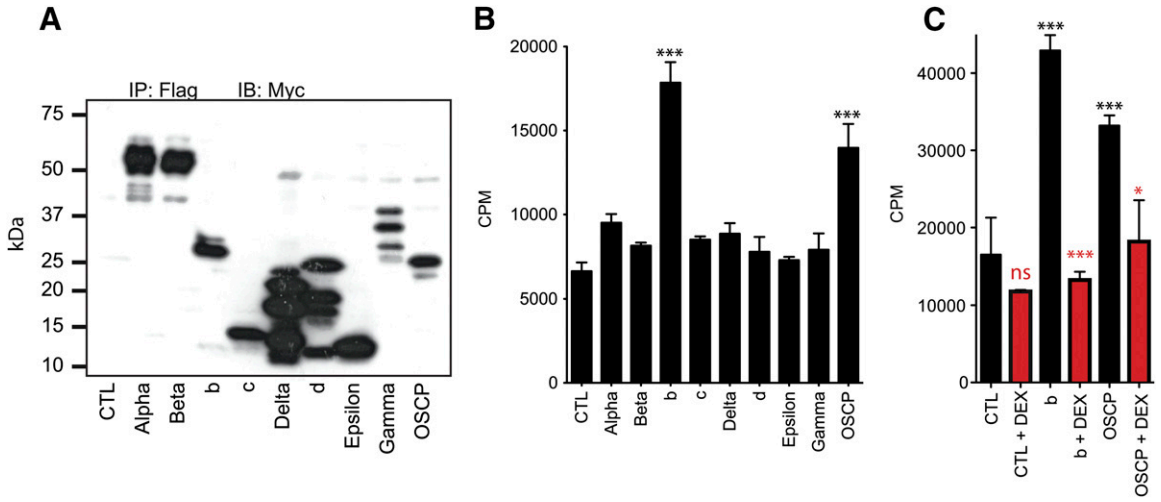

Fig. 5. Evidence for [^{14}C]DEX binding to isolated complex V subunits. (A) Recombinant human F_1F_O ATP synthase subunits purified from mammalian cell expression system. Myc-Flag–tagged constructs for human F_1F_O ATP synthase subunits (as labeled at bottom of gel) immunoprecipitated with anti-Flag affinity gel and immunoblotted with anti-Myc tag antibody. Control (CTL) lane represents immunoprecipitate with anti-Flag affinity gel of cell lysate from nontransfected cells. (B) Counts per minute of anti-Flag affinity gel immunoprecipitates from cells expressing the indicated constructs exposed to 200 nM ^{14}C-labeled DEX. One-way ANOVA, Bonferroni-corrected preplanned post hoc comparisons; $^{***}P < 0.001$. (C) Counts per minute of anti-Flag affinity gel immunoprecipitates from cells exposed to 200 nM ^{14}C-labeled DEX and 20 μM unlabeled ("cold") DEX. One-way ANOVA, Bonferroni-corrected preplanned post hoc comparisons. $^{*}P < 0.05$; $^{***}P < 0.001$; black asterisks are levels of significance for comparisons between control and radiolabeled b and OSCP; red asterisks are levels of significance for comparisons between levels of binding of radiolabeled DEX in b or OSCP columns and levels in the presence of excess unlabeled DEX. ns, not significant.

The slow loss of neurons in these diseases suggests that the contribution of mitochondrial dysfunction to neuronal death involves increasing and cumulative risk of death, rather than acute and immediate causation, as seen with mitochondrial-induced apoptosis (Youle and Strasser, 2008). This suggests that a final common pathway for neuronal degeneration may be energy insufficiency, and an increased understanding of normal and pathologic mitochondrial metabolic regulation may provide significant insights into therapeutic approaches for the treatment of these diseases (Khatri and Man, 2013). The lack of compounds demonstrated to provide benefit in neurodegenerative disease has hampered this effort, inasmuch as a lack of tools has precluded effective experimental approaches.

Recently, we demonstrated that the neuroprotective compound DEX inhibited stress- and injury-induced large-conductance currents in whole, brain-derived mitochondria (Alavian et al., 2012). Additionally, in cultured cells and neurons in culture, DEX enhanced bioenergetic efficiency (Alavian et al., 2012). Specifically, cells incubated in DEX were protected against disease-relevant stressors and had reduced oxygen consumption rates while concomitantly maintaining or increasing cellular ATP levels. While these and other previous experiments indicated that the most likely site of action of the compound was mitochondrial (Alavian et al., 2012), the molecular substrate of these effects remained completely unknown.

We have previously shown that intermediate- and large-conductance channel activity is present at higher frequency in mitochondria isolated from affected brain regions of rodents exposed in vivo to global ischemic injury (Ofengeim et al., 2012), an acute neurologic insult (Ofengeim et al., 2012; Park et al., 2014). Previous studies have suggested that the ischemia channel comprises a complex of proteins including a divalent-sensitive component, Bcl-xL, and voltage-dependent anion channel (Jonas et al., 2004; Miyawaki et al., 2008; Ofengeim et al., 2012). More recently, we determined that a channel sensitive to Bcl-xL resides within the c-subunit of the ATP synthase and has features in common with the mPTP. We determined that components of the F_1 including the β-subunit prevent pore opening by positioning themselves over the pore of a leak conductance within the c-subunit ring (Alavian et al., 2011, 2014; Chen et al., 2011). Our model predicts that cyclophilin D, which is known to bind to OSCP (Giorgio et al., 2009), acts on the pore by facilitating the removal of the F_1 from the c-subunit in a CsA-sensitive manner during pore opening (Alavian et al., 2014). Because DEX binds in a similar configuration to that of CsA, we suggest here that it acts similarly to CsA, although how the exact binding domains within F_1 differ is as yet undetermined.

In support of our model, we showed that the level of bound radiolabeled DEX and current inhibition by DEX were greatly reduced by denaturation or removal of proteins within the F_1 that extend outside the protective lipid bilayer of the inner membrane. Finally, we have shown that radiolabeled DEX binds to the b and OSCP subunits of complex V. These subunits form the stator stalk of complex V and are closely associated with each other, and they would be removed by urea in SMV preparations.

The hypothesis we propose assumes that a leak conductance associated with the mitochondrial inner membrane could lead to shunting of the proton-motive force that provides the energy for oxidative phosphorylation, with negative consequences for bioenergetic efficiency. DEX (and, to the extent tested, CsA) application directly resulted in modulation of ATP synthesis and hydrolysis by mitochondria, and we suggest that the two phenomena, enzymatic modulation and the inner membrane current inhibition by DEX and CsA, are related and result from an interaction with complex V. Specifically, it is possible that the small levels of direct

modulation of enzyme function observed in the presence of DEX reflect a conformational change resulting from the interaction of the drug with complex V. It is unclear which aspect of this action of DEX could prove more relevant to its cellular effects, namely its direct action on enzymatic function or its effect on the associated conductance pathway. It is likely that both will lead to neuroprotection. Regardless, increased or unchanged ATP levels were observed in neurons and other cells after exposure to DEX, accompanied by lower basal oxygen consumption rates (Alavian et al., 2012). This suggests that metabolic protection or even improvement may indeed be a previously unanticipated outcome of enhanced mPTP closure. In the future, drugs that target this channel specifically, potently, and effectively may prove useful in neurodegenerative diseases.

Authorship Contributions

Participated in research design: Alavian, Dworetzky, Bonanni, Sacchetti, Li, Signore, Smith, Gribkoff, Jonas.

Conducted experiments: Alavian, Dworetzky, Bonanni, Zhang, Sacchetti, Li, Signore, Smith, Gribkoff, Jonas.

Contributed new reagents or analytic tools: Dworetzky, Signore, Gribkoff.

Performed data analysis: Alavian, Dworetzky, Bonanni, Sacchetti, Gribkoff, Jonas.

Wrote or contributed to the writing of the manuscript: Alavian, Gribkoff, Jonas.

References

Alavian KN, Beutner G, Lazrove E, Sacchetti S, Park HA, Licznerski P, Li H, Nabili P, Hockensmith K, and Graham M et al. (2014) An uncoupling channel within the c-subunit ring of the F1FO ATP synthase is the mitochondrial permeability transition pore. *Proc Natl Acad Sci USA* **111**:10580–10585.

Alavian KN, Dworetzky SI, Bonanni L, Zhang P, Sacchetti S, Mariggio MA, Onofrj M, Thomas A, Li H, and Mangold JE et al. (2012) Effects of dexpramipexole on brain mitochondrial conductances and cellular bioenergetic efficiency. *Brain Res* **1446**: 1–11.

Alavian KN, Li H, Collis L, Bonanni L, Zeng L, Sacchetti S, Lazrove E, Nabili P, Flaherty B, and Graham M et al. (2011) Bcl-xL regulates metabolic efficiency of neurons through interaction with the mitochondrial F1FO ATP synthase. *Nat Cell Biol* **13**:1224–1233.

Albers DS and Beal MF (2000) Mitochondrial dysfunction and oxidative stress in aging and neurodegenerative disease. *J Neural Transm Suppl* **59**:133–154.

Bernardi P (2013) The mitochondrial permeability transition pore: a mystery solved? *Front Physiol* **4**:95.

Bonanni L, Chachar M, Jover-Mengual T, Li H, Jones A, Yokota H, Ofengeim D, Flannery RJ, Miyawaki T, and Cho CH et al. (2006) Zinc-dependent multiconductance channel activity in mitochondria isolated from ischemic brain. *J Neurosci* **26**:6851–6862.

Bozik ME, Mather JL, Kramer WG, Gribkoff VK, and Ingersoll EW (2011) Safety, tolerability, and pharmacokinetics of KNS-760704 (dexpramipexole) in healthy adult subjects. *J Clin Pharmacol* **51**:1177–1185.

Brand MD (2005) The efficiency and plasticity of mitochondrial energy transduction. *Biochem Soc Trans* **33**:897–904.

Cassarino DS, Fall CP, Smith TS, and Bennett JP, Jr (1998) Pramipexole reduces reactive oxygen species production in vivo and in vitro and inhibits the mitochondrial permeability transition produced by the parkinsonian neurotoxin methylpyridinium ion. *J Neurochem* **71**:295–301.

Caviston TL, Ketchum CJ, Sorgen PL, Nakamoto RK, and Cain BD (1998) Identification of an uncoupling mutation affecting the b subunit of F1F0 ATP synthase in Escherichia coli. *FEBS Lett* **429**:201–206.

Chan TL, Greenawalt JW, and Pedersen PL (1970) Biochemical and ultrastructural properties of a mitochondrial inner membrane fraction deficient in outer membrane and matrix activities. *J Cell Biol* **45**:291–305.

Chaturvedi RK and Beal MF (2008) Mitochondrial approaches for neuroprotection. *Ann N Y Acad Sci* **1147**:395–412.

Chen YB, Aon MA, Hsu YT, Soane L, Teng X, McCaffery JM, Cheng WC, Qi B, Li H, and Alavian KN et al. (2011) Bcl-xL regulates mitochondrial energetics by stabilizing the inner membrane potential. *J Cell Biol* **195**:263–276.

Chouhan AK, Ivannikov MV, Lu Z, Sugimori M, Llinas RR, and Macleod GT (2012) Cytosolic calcium coordinates mitochondrial energy metabolism with presynaptic activity. *J Neurosci* **32**:1233–1243.

Courchet J, Lewis TL, Jr, Lee S, Courchet V, Liou DY, Aizawa S, and Polleux F (2013) Terminal axon branching is regulated by the LKB1-NUAK1 kinase pathway via presynaptic mitochondrial capture. *Cell* **153**:1510–1525.

Damiano M, Starkov AA, Petri S, Kipiani K, Kiaei M, Mattiazzi M, Flint Beal M, and Manfredi G (2006) Neural mitochondrial Ca2+ capacity impairment precedes the onset of motor symptoms in G93A Cu/Zn-superoxide dismutase mutant mice. *J Neurochem* **96**:1349–1361.

David G and Barrett EF (2003) Mitochondrial Ca2+ uptake prevents desynchronization of quantal release and minimizes depletion during repetitive stimulation of mouse motor nerve terminals. *J Physiol* **548**:425–438.

Dejean LM, Martinez-Caballero S, Guo L, Hughes C, Teijido O, Ducret T, Ichas F, Korsmeyer SJ, Antonsson B, and Jonas EA et al. (2005) Oligomeric Bax is a component of the putative cytochrome c release channel MAC, mitochondrial apoptosis-induced channel. *Mol Biol Cell* **16**:2424–2432.

Elrod JW and Molkentin JD (2013) Physiologic functions of cyclophilin D and the mitochondrial permeability transition pore. *Circ J* **77**:1111–1122.

Giorgio V, Bisetto E, Soriano ME, Dabbeni-Sala F, Basso E, Petronilli V, Forte MA, Bernardi P, and Lippe G (2009) Cyclophilin D modulates mitochondrial F0F1-ATP synthase by interacting with the lateral stalk of the complex. *J Biol Chem* **284**: 33982–33988.

Glater EE, Megeath LJ, Stowers RS, and Schwarz TL (2006) Axonal transport of mitochondria requires milton to recruit kinesin heavy chain and is light chain independent. *J Cell Biol* **173**:545–557.

Gribkoff VK and Bozik ME (2008) KNS-760704 [(6R)-4,5,6,7-tetrahydro-N6-propyl-2, 6-benzothiazole-diamine dihydrochloride monohydrate] for the treatment of amyotrophic lateral sclerosis. *CNS Neurosci Ther* **14**:215–226.

Gu M, Iravani MM, Cooper JM, King D, Jenner P, and Schapira AH (2004) Pramipexole protects against apoptotic cell death by non-dopaminergic mechanisms. *J Neurochem* **91**:1075–1081.

Jonas EA, Hickman JA, Chachar M, Polster BM, Brandt TA, Fannjiang Y, Ivanovska I, Basañez G, Kinnally KW, and Zimmerberg J et al. (2004) Proapoptotic N-truncated BCL-xL protein activates endogenous mitochondrial channels in living synaptic terminals. *Proc Natl Acad Sci USA* **101**:13590–13595.

Jonas EA, Porter GA, and Alavian KN (2014) Bcl-xL in neuroprotection and plasticity. *Front Physiol* **5**:355.

Khatri N and Man HY (2013) Synaptic activity and bioenergy homeostasis: implications in brain trauma and neurodegenerative diseases. *Front Neurol* **4**:199.

Kirichok Y, Krapivinsky G, and Clapham DE (2004) The mitochondrial calcium uniporter is a highly selective ion channel. *Nature* **427**:360–364.

Ko YH, Delannoy M, Hullihen J, Chiu W, and Pedersen PL (2003) Mitochondrial ATP synthasome. Cristae-enriched membranes and a multiwell detergent screening assay yield dispersed single complexes containing the ATP synthase and carriers for Pi and ADP/ATP. *J Biol Chem* **278**:12305–12309.

Li H, Chen Y, Jones AF, Sanger RH, Collis LP, Flannery R, McNay EC, Yu T, Schwarzenbacher R, and Bossy B et al. (2008) Bcl-xL induces Drp1-dependent synapse formation in cultured hippocampal neurons. *Proc Natl Acad Sci USA* **105**: 2169–2174.

Lötscher HR, deJong C, and Capaldi RA (1984) Interconversion of high and low adenosinetriphosphatase activity forms of Escherichia coli F1 by the detergent lauryldimethylamine oxide. *Biochemistry* **23**:4140–4143.

Miyawaki T, Mashiko T, Ofengeim D, Flannery RJ, Noh KM, Fujisawa S, Bonanni L, Bennett MV, Zukin RS, and Jonas EA (2008) Ischemic preconditioning blocks BAD translocation, Bcl-xL cleavage, and large channel activity in mitochondria of postischemic hippocampal neurons. *Proc Natl Acad Sci USA* **105**:4892–4897.

Nguyen PV, Marin L, and Atwood HL (1997) Synaptic physiology and mitochondrial function in crayfish tonic and phasic motor neurons. *J Neurophysiol* **78**: 281–294.

Nicholls DG (2008) Oxidative stress and energy crises in neuronal dysfunction. *Ann N Y Acad Sci* **1147**:53–60.

Ofengeim D, Chen YB, Miyawaki T, Li H, Sacchetti S, Flannery RJ, Alavian KN, Pontarelli F, Roelofs BA, and Hickman JA et al. (2012) N-terminally cleaved Bcl-xL mediates ischemia-induced neuronal death. *Nat Neurosci* **15**:574–580.

O'Rourke B (2004) Evidence for mitochondrial K+ channels and their role in cardioprotection. *Circ Res* **94**:420–432.

O'Rourke B (2007) Mitochondrial ion channels. *Annu Rev Physiol* **69**:19–49.

Park HA, Licznerski P, Alavian KN, Shanabrough M, and Jonas EA (2014) Bcl-xL is necessary for neurite outgrowth in hippocampal neurons. *Antioxid Redox Signal* DOI: 10.1089/ars.2013.5570 [published ahead of print].

Pavlov EV, Priault M, Pietkiewicz D, Cheng EH, Antonsson B, Manon S, Korsmeyer SJ, Mannella CA, and Kinnally KW (2001) A novel, high conductance channel of mitochondria linked to apoptosis in mammalian cells and Bax expression in yeast. *J Cell Biol* **155**:725–731.

Pedersen PL, Hullihen J, and Wehrle JP (1981) Proton adenosine triphosphatase complex of rat liver. The effect of trypsin on the F1 and F0 moieties of the enzyme. *J Biol Chem* **256**:1362–1369.

Petronilli V, Szabò I, and Zoratti M (1989) The inner mitochondrial membrane contains ion-conducting channels similar to those found in bacteria. *FEBS Lett* **259**:137–143.

Raffaello A, De Stefani D, Sabbadin D, Teardo E, Merli G, Picard A, Checchetto V, Moro S, Szabò I, and Rizzuto R (2013) The mitochondrial calcium uniporter is a multimer that can include a dominant-negative pore-forming subunit. *EMBO J* **32**:2362–2376.

Rao VK, Carlson EA, and Yan SS (2014) Mitochondrial permeability transition pore is a potential drug target for neurodegeneration. *Biochim Biophys Acta* **1842**: 1267–1272.

Sacchetti S, Alavian KN, Lazrove E, and Jonas EA (2013) F1FO ATPase vesicle preparation and technique for performing patch clamp recordings of submitochondrial vesicle membranes. *J Vis Exp* **75**:e4394 DOI: 10.3791/4394.

Sayeed I, Parvez S, Winkler-Stuck K, Seitz G, Trieu I, Wallesch CW, Schönfeld P, and Siemen D (2006) Patch clamp reveals powerful blockade of the mitochondrial permeability transition pore by the D2-receptor agonist pramipexole. *FASEB J* **20**: 556–558.

Sheng ZH (2014) Mitochondrial trafficking and anchoring in neurons: new insight and implications. *J Cell Biol* **204**:1087–1098.

Sun T, Qiao H, Pan PY, Chen Y, and Sheng ZH (2013) Motile axonal mitochondria contribute to the variability of presynaptic strength. *Cell Reports* **4**:413–419.

Szabó I, Bernardi P, and Zoratti M (1992) Modulation of the mitochondrial megachannel by divalent cations and protons. *J Biol Chem* **267**:2940–2946.
Szabó I and Zoratti M (1991) The giant channel of the inner mitochondrial membrane is inhibited by cyclosporin A. *J Biol Chem* **266**:3376–3379.
Watt IN, Montgomery MG, Runswick MJ, Leslie AG, and Walker JE (2010) Bioenergetic cost of making an adenosine triphosphate molecule in animal mitochondria. *Proc Natl Acad Sci USA* **107**:16823–16827.
Youle RJ and Strasser A (2008) The BCL-2 protein family: opposing activities that mediate cell death. *Nat Rev Mol Cell Biol* **9**:47–59.
Zorov DB, Filburn CR, Klotz LO, Zweier JL, and Sollott SJ (2000) Reactive oxygen species (ROS)-induced ROS release: a new phenomenon accompanying induction of the mitochondrial permeability transition in cardiac myocytes. *J Exp Med* **192**:1001–1014.

Address correspondence to: Elizabeth A. Jonas, Department of Internal Medicine, Yale University School of Medicine, P.O. Box 208020, New Haven, CT 06530. E-mail: Elizabeth.jonas@yale.edu